

Soft tetragonal distortions in ferromagnetic Ni_2MnGa and related materials from first principles

V.V. Godlevsky and K. M. Rabe

Department of Physics and Astronomy,

Rutgers University, 136 Frelinghuysen Rd, Piscataway, NJ 08854

(October 25, 2018)

A detailed examination of the energy landscape, density of states and magnetic moment of tetragonally distorted ferromagnetic Ni_2MnGa was performed using first-principles local-spin-density (LSD) pseudopotential calculations, varying V as well as c/a . The energy of tetragonal Ni_2MnGa is found to be *nearly constant* for values of c/a over a wide range, with shallow minima near $c/a = 1$ and 1.08 in addition to that near 1.2. This flat energy surface is consistent with the wide range of observed values of c/a . It also explains the observation of pseudomorphic growth of Ni_2MnGa on GaAs, despite a nominal 3% lattice mismatch. The related materials Ni_2MnAl , Ni_2MnIn and ferromagnetic NiMn were examined for similar behavior, but all are seen to have a single well-defined minimum at c/a near 1, consistent with available experimental information. For NiMn, the ground state antiferromagnetic ordering and structural parameters are correctly predicted within the LSD approach.

71.15.Nc,81.30.Kf,75.50.-y

In the design of mechanical actuator devices, both on macroscopic scales and in thin-film based MEMS, there is continuing interest in identifying and optimizing new high-performance materials. Materials which exhibit a martensitic transformation and associated shape memory effect have been shown to be quite useful, though their high-frequency applications are limited by the slow rate of the martensitic transformation and poor energy conversion. It has been proposed¹ that this deficiency could be addressed by using shape memory materials which are ferromagnetic, and using applied magnetic fields to control the mechanical response²⁻⁴.

Therefore, it is of particular interest to identify candidate ferromagnetic martensites and to understand the transition mechanism, especially the coupling between magnetic and structural degrees of freedom. The rather small number of known systems includes Fe-Pt, Co-Ni, Fe-Mn-C, Fe-Ni-C, Fe-Ni-Co-Ti and Fe-Ni, with the Heusler structure compound Ni_2MnGa being the most thoroughly investigated to date⁴⁻¹⁰.

In this paper, we investigate the structural energetics of Ni_2MnGa and related materials from first principles, with a particular focus on the tetragonal distortion associated with the martensitic transition. For comparison, we examine Ni_2MnAl and Ni_2MnIn (not observed to be martensitic), and NiMn, related by replacing Ga with an additional Mn (exhibits a martensitic transition to an antiferromagnetic tetragonal phase¹¹). While our calculations are for bulk crystals, they also allow us to predict the effects of epitaxial stress, which often is the dominant factor in determining the structure and properties of thin films.

We use the self-consistent pseudopotential plane wave approach¹² within the local spin density approximation (LSDA). We use Troullier-Martins¹³ pseudopotentials and exchange and correlation potential in the Perdew-

TABLE I. Reference configurations and cut-off radii (a.u.) used to construct the pseudopotentials.

	r_s	r_p	r_d
Ni $3d^8 4s^2 4p^0$	2.2	2.2	2.2
Mn $3d^5 4s^2 4p^0$	1.9	2.6	2.0
Al $4s^2 4p^1 4d^0$	2.3	2.3	2.3
Ga $4s^2 4p^1 4d^0$	3.0	2.6	3.0
In $4s^2 4p^1 4d^0$	3.0	3.0	3.0

Wang¹⁴ form. The nonlinear core correction scheme¹⁵ was used in the construction of the pseudopotentials. The pseudopotential cut-off radii are summarized in Table I. The local components of the pseudopotentials¹⁶ are chosen to be $l=0$ for Ni, Mn, Al and In and $l=1$ for Ga. The energy plane-wave cut-off is 70 Ry. The unit cells consist of one formula unit for Ni_2MnX ($X = \text{Al, Ga, and In}$) and two formula units for NiMn. The Brillouin zone is sampled by a $10 \times 10 \times 10$ k-point Monkhorst-Pack (MP)¹⁷ mesh with zero shift. To be able to calculate the magnetic moment accurately, we do not apply temperature smearing for the k-point integration. In NiMn, we studied two antiferromagnetic phases: AF-I, with the Mn atoms with parallel moments located on alternating $(1\ 1\ 0)$ planes; and AF-II, with parallel moments on alternating $(1\ 1\ \bar{1})$ planes (in the cubic reference system)¹⁸. The self-consistent calculations tend to converge to a local ferromagnetic minimum. To make the system converge to the antiferromagnetic state, approximately 0.2 eV/atom lower in energy, we constrain the total magnetic moment to zero.

For the high temperature cubic structures, our calculations yield the lattice constants, bulk moduli and mag-

TABLE II. Lattice constants, bulk moduli and magnetic moments of Ni₂MnX compounds (L₂₁ structure) and FM-NiMn (B2 structure) compared to experiment (in parentheses) and previous theoretical calculations (square brackets), where available.

a (a.u.)	
FM-NiMn	5.56 (5.63 ^a)
Ni ₂ MnAl	10.93 (11.01 ^b) [10.98 ^d]
Ni ₂ MnGa	10.91 (11.01 ^b) [10.95 ^d]
Ni ₂ MnIn	11.32 (11.47 ^b) [11.43 ^e]
B (GPa)	
FM-NiMn	155
Ni ₂ MnAl	167 [163 ^d]
Ni ₂ MnGa	170 (146 ^c) [156 ^d]
Ni ₂ MnIn	138
$\mu(\mu_B/Mn)$	
FM-NiMn	4.42 [3.8 ^g]
Ni ₂ MnAl	4.22 (4.19 ^b) [4.03 ^d]
Ni ₂ MnGa	4.22 (4.17 ^b) [4.09 ^d]
Ni ₂ MnIn	4.31 (4.40 ^b) [3.91 ^e] [4.16 ^f]

^aReference 19

^bReference 6

^cReference 20

^dReference 5

^eReference 32

^fReference 31

^gReference 18

netic moments given in Table II. For NiMn, we compare calculated results for a hypothetical ferromagnetic cubic phase with measurements in the paramagnetic cubic phase. The results compare well with experiment and with previous first-principles studies.

Next, we present the results of total energy calculations for uniform tetragonal distortions of these cubic structures, and discuss them in the context of observed low-symmetry phases. At least three distinct ferromagnetic low-symmetry phases have been experimentally observed in bulk Ni₂MnGa⁷, two tetragonal (β' and β''') and one orthorhombic (β''). The β' phase, obtained by cooling of the high-temperature Heusler (L₂₁) phase below $T_m \approx 200$ K, has a tetragonal structure with $c/a = 0.94$ ($a=5.920$ Å and $c=5.566$ Å).⁶ The relative volume change across the martensitic transition is only 1%. In addition, there is a shuffle of the (1 1 0) planes along [110]. This has incommensurate periodicity represented by a wavevector of $\pi/a[0.43,0.43,0]$, corresponding to approximately five interplanar distances^{8,9}. The transition is preceded by a cubic premartensitic ($L2_{PM}$) phase below $T_{PM} \approx 260$ K, characterized by softening and condensation of transverse acoustic phonons $\pi/a[0.33,0.33,0]$ with displacements similar in type to the shuffle distortion below T_m . Under uniaxial compression along [1 1 0] the β' phase transforms into the orthorhombic β'' phase

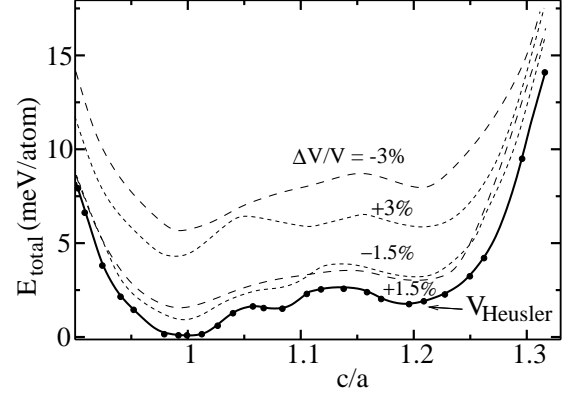


FIG. 1. Total energy as a function of c/a in Ni₂MnGa. Each curve corresponds to a constant volume V per unit cell, measured relative to $V_{Heusler} = 1300$ a.u.³ The curves are separated by intervals of $\Delta V/V = 1.5\%$. Each curve represents an interpolation through 26 points, shown explicitly by filled circles for $V = V_{Heusler}$.

($a = 5.54$ Å, $b = 5.78$ Å and $c = 6.12$ Å)⁷. X-ray analysis shows that β''' martensite is also modulated with [110] displacements of the (1 1 0) planes with a periodicity of seven (1 1 0) interplanar distances. The third martensite phase β''' , obtained by further compression along [1 1 0], is metastable with respect to the removal of the applied stress⁷. The β''' structure is a uniform tetragonal distortion of the cubic Heusler structure ($a = 6.44$ Å and $c = 5.52$ Å) with $c/a = 1.18$. The relationships between these phases can be summarized as follows:

$$L2_1 \xrightarrow{T=260K} L2_{PM} \xrightarrow{T=200K} \beta' \xrightarrow{[110] \text{ stress}} \beta'' \xrightarrow{[110] \text{ stress}} \beta''' \quad (1)$$

The calculated energy of Ni₂MnGa as a function of c/a for $V = V_{Heusler}$ is shown in Figure 1. The region of c/a from 0.9 to 1.3 is examined in considerable detail, with 26 separate calculations. Based on the experimental observations of bulk crystal structures, one would expect to find a local minimum in the energy as a function of c/a near 1.18 and perhaps another near 0.94. There is a shallow low-energy local minimum near $c/a = 1.19$ with total energy 2 meV/atom higher than the L₂₁ structure. In the previous calculations of Ayuela *et.al.*, this minimum is at $c/a=1.16$ and is slightly lower in energy than the L₂₁ structure. The minimum can readily be associated with the pure tetragonal β''' phase observed by Kokorin *et.al.* with $c/a=1.18$ ⁷. In contrast, there is no local minimum or any discernible anomaly at $c/a = 0.94$, with a smooth decrease to the minimum at the L₂₁ structure. However, our fine-scale exploration of the energy surface does reveal that the entire energy surface for $0.95 < c/a < 1.25$ is remarkably flat, with the total energy varying

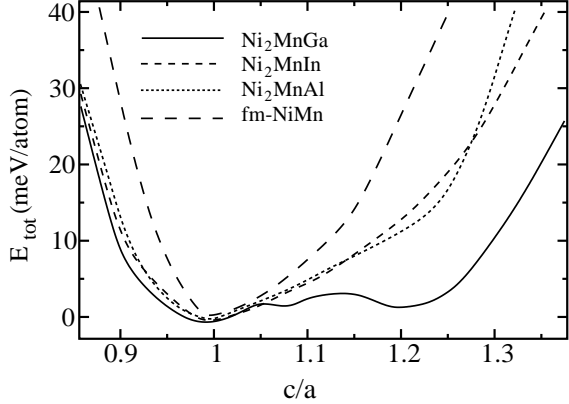


FIG. 2. Total energy as a function of c/a ratio of several related compounds, compared with Ni_2MnGa . The curve for each compound is computed at a constant volume equal to the theoretical V_{Heusler} given in Table II. Each curve represents an interpolation through at least 20 points in the range shown. The energies are given relative to the energy at $c/a = 1$, with the curves slightly offset for clarity.

less than 2.5 meV/atom. This has significant physical consequences for thin films which will be discussed further below.

First, we consider the reasons for the absence of a local minimum corresponding to the ground state β' phase. It has been suggested that the tetragonal distortion could be stabilized by a change in volume⁵. To investigate this hypothesis, we computed the energy as a function of c/a for varying volumes, with results shown in Figure 1. We sampled the volumes in 1.5% increments of $\Delta V/V$. Even with the possibility of volume change, the $L2_1$ structure remains the total energy minimum, with no local minimum corresponding to the β' structure. We remark that the minimum near $c/a = 1.19$ is lowered relative to the cubic structure as V increases, although it never actually becomes more favorable. We have also calculated the total energy of a pure orthorhombic structure at the experimental lattice constants, which give $c/a=1.11$ and $b/a=1.04$.⁷ The calculated energy of this orthorhombic phase is 4 meV per atom higher than the $L2_1$ phase, consistent with previous calculations.⁵ We conclude that the observed shuffle distortions are crucial to stabilizing the observed β' and β'' phases.

A number of related materials were examined for comparison. Martensitic transitions have been observed in the Ni-Mn-Al system, but not in stoichiometric Ni_2MnAl ^{30,29}. Similarly, there are no reports of low-symmetry phases of Ni_2MnIn . NiMn exhibits a martensitic transition from a cubic paramagnetic phase at $T_m = 943$ K to a tetragonal phase with $c/a = 1.33$ which, however, is *antiferromagnetic*^{11,19}.

For Ni_2MnAl , Ni_2MnIn , and ferromagnetic NiMn, the

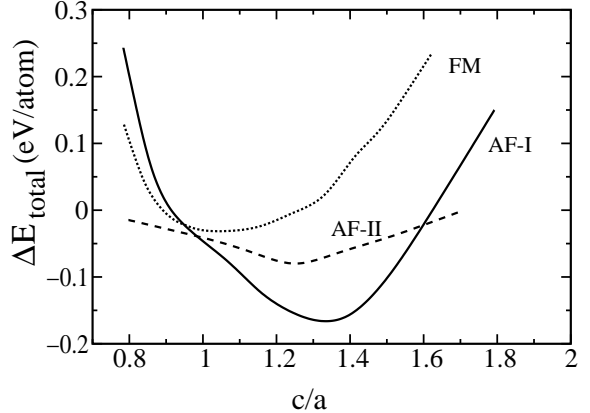


FIG. 3. Total energy of NiMn (FM, AF-I, AF-II phases) as a function of c/a at constant volume. For FM, AF-I and AF-II phases, we chose the volume of the observed experimental structure^{11,19}, $a=3.74$ Å and $c=3.52$ Å.

energy as a function of c/a for $V = V_{\text{Heusler}}$ is shown in Figure 2. All three compounds are seen to have a single well-defined minimum at c/a near 1, consistent with available experimental information. In the previous calculations of Ayuela *et.al.*, there was another metastable minimum for Ni_2MnAl at $c/a=1.22$. We find that for Ni_2MnAl the shape of this curve is very sensitive to the k -point sampling density, with a local minimum near $c/a=1.2$ evolving into a slope “discontinuity” for grids denser than $8 \times 8 \times 8$.

When constrained to be ferromagnetic, NiMn has a tetragonal distortion energy curve similar in shape to that of Ni_2MnIn and Ni_2MnAl , though with a larger stiffness. The substitution of a magnetic atom in the X site has, however, significant consequences for the magnetic order, stabilizing a type-I antiferromagnetically ordered structure (AF-I) by 190 meV over the lowest-energy ferromagnetic structure (FM). This is in good agreement with the value of 200 meV obtained in a previous calculation¹⁸, performed with lattice constants fixed at experimental values. As shown in Figure 3, total energy minimization for the AF-I NiMn structure leads to a predicted value of $c/a = 1.33$, consistent with experiment.^{11,19} At this value a pseudogap appears at the Fermi level, as shown in Figure 4. As the tetragonal distortion deviates from $c/a = 1.33$ the pseudogap becomes less pronounced and finally Ni d-states fill the gap. The formation of a pseudogap and the associated enhanced stability does not appear for a distinct antiferromagnetic ordering (AF-II), which is higher in energy by 70 meV and has a much shallower minimum at $c/a = 1.24$.

The densities of states for cubic Ni_2MnX ($X = \text{Ga}, \text{Al}$ and In) are shown in Figure 5. For all three compounds, these are quite similar, especially near the Fermi level. The total magnetic moment of Ni_2MnGa $L2_1$ structure is

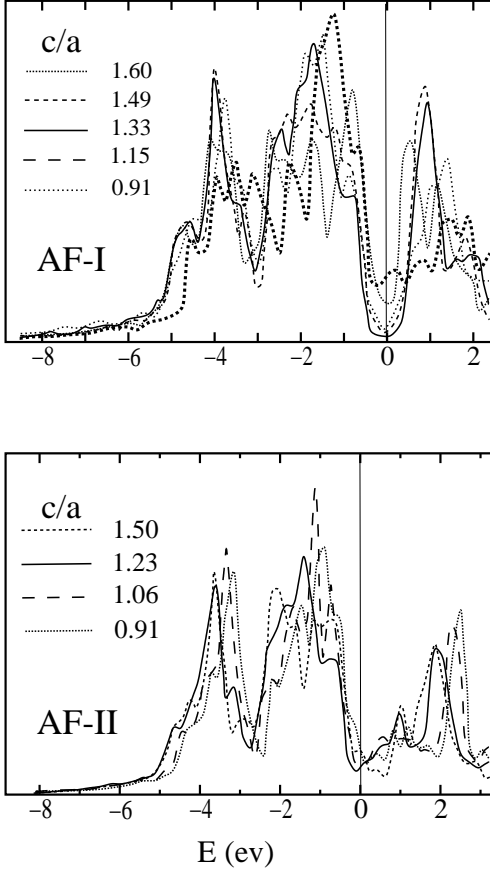


FIG. 4. Density of states for (a) the AF-I and (b) the AF-II phases of NiMn for varying c/a at the same volume as in Figure 3. The solid line corresponds to the minimum energy states for both AF-I and AF-II phases.

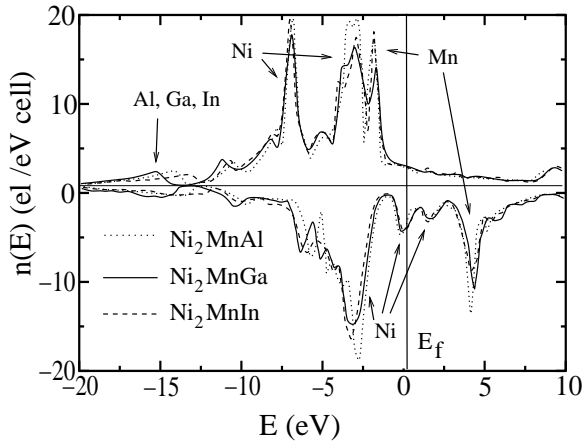


FIG. 5. Density of states in Ni_2MnX compounds ($X = \text{Al}, \text{Ga}, \text{In}$). The atomic character (obtained by projecting the wave functions onto individual atoms) is indicated by appropriate labels.

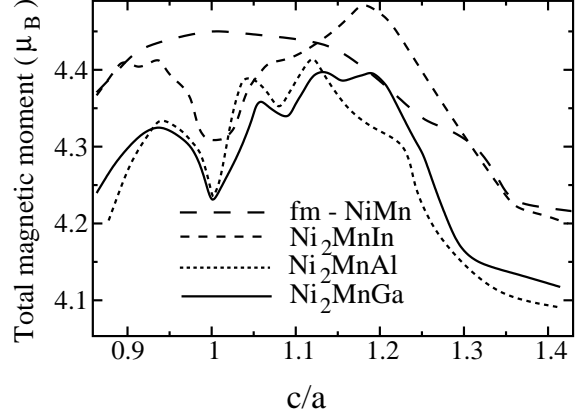


FIG. 6. Total magnetic moments of Ni_2MnX ($X = \text{Al}, \text{Ga}, \text{In}$) and FM-NiMn as a function of c/a , corresponding to the total energy calculations in Figure 2.

$4.228 \mu_B$, which decomposes into $0.301/3.700/-0.075 \mu_B$ on Ni/Mn/Ga atoms. This agrees well with the previous calculations of References 5 and 10.

The magnetic moment as a function of c/a , shown in Figure 6, is again similar for all three compounds. It shows a sharp minimum at c/a near 1 and a local maximum at $c/a \approx 0.94$. From the atomic decomposition of this curve for Ni_2MnGa in Figure 7, we see that the features can be directly attributed to the Ni contribution, most likely associated with a small Ni-derived peak in the minority density of states located just below the Fermi level. It is interesting to note that the position of this maximum coincides with the value of c/a for the β' martensitic structure.

The softness of the tetragonal distortion in Ni_2MnGa has significant implications for the growth and properties of thin films. Efforts to grow single-crystal thin films on a GaAs substrate (with 3.1% lattice mismatch) have been carried out by MBE^{26,27}. Using a $\text{Sc}_{0.3}\text{Er}_{0.7}\text{As}$ interlayer, a tetragonal-structure film with lattice parameters $a = 0.565 \text{ nm}$ and $c = 0.612 \text{ nm}$ was obtained. This is exactly the structure we expect based on the total energy curves in Fig. 1. As the in-plane a is reduced to 0.565 nm to match the substrate, the c axis increases to maintain the volume of the cubic Heusler phase, which minimizes the total energy over the whole range of c/a considered. The energy of the resulting structure, at $c/a = 1.08$, is less than 2 meV/atom higher than the cubic structure, explaining the observation that the thickness of this pseudomorphic film, 300 \AA , far exceeds the critical thickness expected for the given lattice mismatch. While the large epitaxial stress should affect the structure and properties significantly, if the film can be released it should exhibit a martensitic transition and shape-memory properties.

In another recent experiment²⁷ a 450 \AA thick film of Ni_2MnGa was grown by MBE on a GaAs substrate using

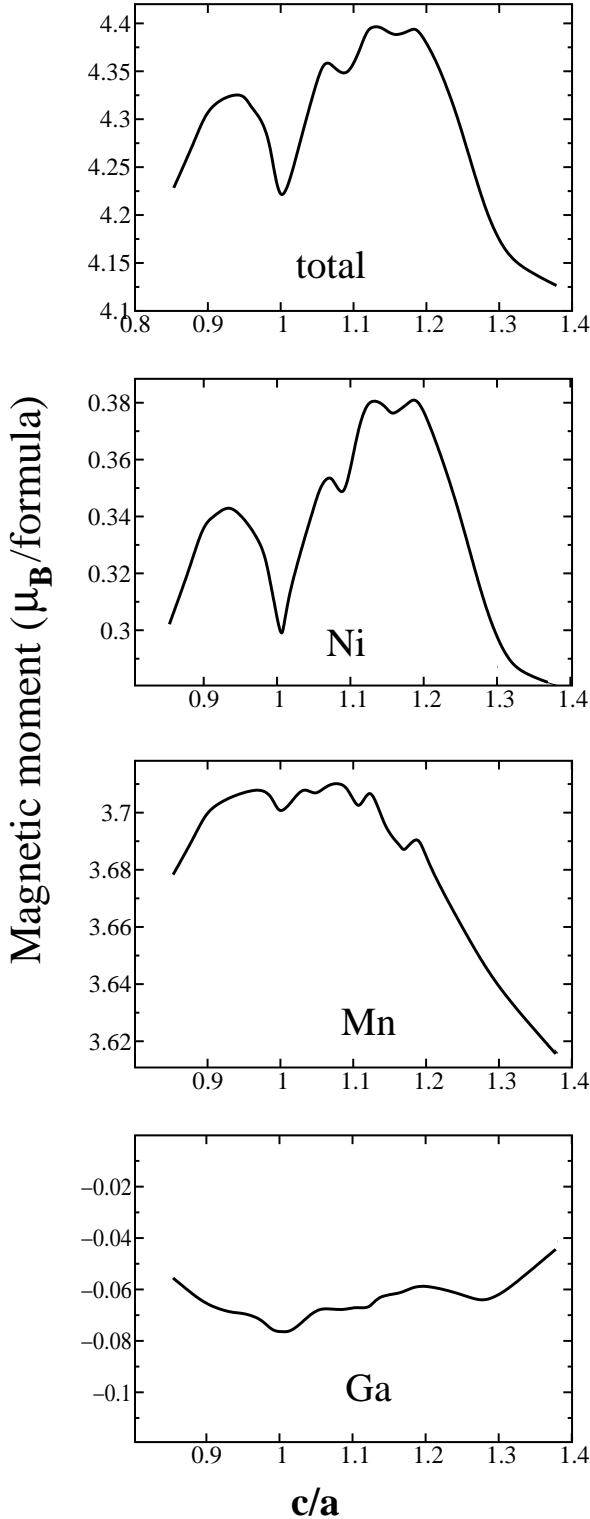


FIG. 7. Total magnetic moment and contributions associated with individual elements atoms in Ni_2MnGa as a function of c/a for $V = V_{\text{Heusler}}$. Note the difference in the vertical scale between the first plot and subsequent plots.

a NiGa interlayer. The structure of this film was reported to be tetragonal, with $c/a = 1.05$ ($a=5.79 \text{ \AA}$ and $c=6.07 \text{ \AA}$). In this case, the lattice constant of Ni_2MnGa is a close (0.6%) match to the interlayer, leading to the expectation that the structure of the film should be cubic. Instead, the c parameter is expanded, resulting in a volume 3% larger than the volume of the $L2_1$ structure. One explanation might be a slight change in the stoichiometry of the film. Modelling the effect of this shift as a negative applied hydrostatic pressure, we now focus on the $\Delta V/V = +3\%$ curve in 1. The flatness of this curve is similar to that for $V = V_{\text{Heusler}}$. Thus, although the expanded system is formally mismatched to the NiGa interlayer, the constraint $a = 5.79 \text{ \AA}$ is associated with an energy cost of less than 2 meV/atom, which would allow pseudomorphic growth of this tetragonal film far beyond the critical thickness.

This study highlights the fact that the energy surface of Ni_2MnGa is far from simple. Studies of additional instabilities of the cubic Heusler structure via density-functional perturbation theory are in progress. In particular, the energies of shuffle distortions as a function of wavevector can be obtained with this method for a better understanding of the observed β' ground state structure. This information will also allow us to model the properties of the high-temperature cubic Heusler phase within an effective Hamiltonian approach. We expect that these properties reflect the presence of large local distortions around the average cubic structure and there should be interesting differences from the properties of other Heusler phases whose ground state structure is cubic.

In conclusion, we performed first principles calculations of the total energy as a function of tetragonal distortion (c/a) and volume V for Ni_2MnGa and related compounds Ni_2MnAl , Ni_2MnIn , and NiMn . The total energy of Ni_2MnGa at constant volume is remarkably flat in the range $0.95 < c/a < 1.25$, varying less than 2.5 meV/atom. This provides an explanation of the surprisingly high compliance of single-crystal films grown by MBE. In contrast, the related materials Ni_2MnAl , Ni_2MnIn , and ferromagnetic NiMn have a single well-defined minimum near $c/a = 1$. The densities of states and c/a dependence of the magnetic moments are quite similar in all compounds studied, leading us to conclude that the unique behavior of Ni_2MnGa is the result of fine tuning. It may be possible to achieve this in other systems through appropriate alloying.

We thank R. D. James, K. Bhattacharya, C.J. Palmström, J. Dong, C. Bungaro, X. Huang and A. Ayuela for valuable discussions. This work was supported by AFOSR/MURI F49620-98-1-0433.

- ¹ R. James and K. Hane, *Acta Materialia* **48**, 197 (2000).
- ² R. James and D. Kinderlehrer, *Phil. Mag. B* **68**, 237 (1993).
- ³ R. James and D. Kinderlehrer, *J. Appl. Phys.* **76**, 7012 (1994).
- ⁴ K. Ullakko, J. Huang, C. Kanter, R. O’Handley, and V. Kokorin, *Appl. Phys. Lett.* **69**, 1966 (1996).
- ⁵ A. Ayuela, J. Enkovaara, K. Ullako and R. Niemnen, *J. Phys: Cond. Matt.* **11**, 2017 (1999).
- ⁶ P. Webster, K. Ziebeck, S. Tows, and M. Peak, *Phil. Mag.* **49**, 295 (1984).
- ⁷ V. V. Kokorin, V. V. Martynov, and V. A. Chernenko, *Scr. Metall. Mater.* **26**, 175 (1992).
- ⁸ A. Zheludev, S. Shapiro, P. Wochner, A. Schwartz, M. Wall, and L. Taner, *Phys. Rev. B* **51**, 11310 (1994).
- ⁹ A. Zheludev, S. Shapiro, A. Vasil’ev, S. Konoplyuk, and E. Khapalyuk, *Phys. Solid State* **37**, 2049 (1995).
- ¹⁰ O. Velikohatnyi and I. Naumov, *Phys. Solid State* **41**, 684 (1999).
- ¹¹ J.S. Kasper and J.S. Kouvel, *J. Phys. Chem. Solids* **11**, 231 (1959).
- ¹² J. Chelikowsky and M. L. Cohen in *“Handbook on Semiconductors”*, vol. 1, ed. P. T. Landsberg (1992).
- ¹³ N. Troullier and J.L. Martins, *Phys. Rev. B* **43**, 1993 (1991).
- ¹⁴ J. Perdew and Y. Wang, *Phys. Rev. B* **45**, 13244 (1992).
- ¹⁵ S. Louie, S. Froyen, and M. L. Cohen, *Phys. Rev. B* **26**, 1738 (1982).
- ¹⁶ L. Kleinman and D. Bylander, *Phys. Rev. Lett.* **48**, 1425 (1982).
- ¹⁷ H. Monkhorst and J. Pack, *Phys. Rev. B* **13**, 5188 (1976).
- ¹⁸ A. Sakuma, *J. of Magn. Magn. Mat.* **187**, 105 (1997).
- ¹⁹ V. Egorushkin, S. Kulkov, and S. Kulkova, *Physica B and C* **123B**, 61 (1983).
- ²⁰ J. Worgull, E. Petti and J. Trivisonno, *Phys. Rev. B* **54**, 15695 (1996).
- ²¹ E. Vintaykin, P. Potapov, and N. Poliakova, *Proc. Conf. MARTENSIT-91*, Kiev, Ukraine, 386 (1992).
- ²² W. Yang and D. Mikkola, *MRS Symp. Proc.* **246**, 135 (1992).
- ²³ P. Potapov and V. Udovenko, *J. de Phys.* **5**, C8-1059 (1996).
- ²⁴ R. James and M. Wuttig, *Phil. Mag. A* **77**, 1273 (1998).
- ²⁵ E. Kren and L. Pal, *J. Phys. Chem. Solids* **26**, 101 (1968).
- ²⁶ J. Dong, L. Chen, C. Palmstrøm, R. James, and S. McKernan, *Appl. Phys. Lett.* **75**, 1443 (1999).
- ²⁷ J. Dong, L. Chen, S. McKernan, J. Xie, M. Figus, R. James, and C. Palmstrøm, to be published in the Proceedings of 1999 MRS Fall Conference, Smart Materials session.
- ²⁸ C. J. Palmstrom, private communication.
- ²⁹ Y. Sutou, I. Ohnuma, R. Kainuma, and K. Ishida, *Metall. Mater. Trans. A* **29**, 2225 (1998).
- ³⁰ F. Gejima, Y. Sutou, R. Kainuma, and K. Ishida, *Metall. Mater. Trans. A* **30**, 2721 (1999).
- ³¹ K. A. Kilian and R. H. Victora, *J. Appl. Phys.* **87**, 7064 (2000).
- ³² E. Z. da Silva, O. Jepsen and O. K. Andersen, *Solid State Comm.* **67**, 13 (1988).